

# Analytical Investigation of Seismic Performance of Exterior RC Beam-Column Joints Rehabilitated with New Scheme

A. Hosseini, M.Marefat, A. Arzeytoon & J. Shafaei

School of Civil Engineering, University of Tehran, Tehran, Iran



## SUMMARY:

Several earthquakes have demonstrated many collapses of buildings due to the brittle failure of sub-standard beam-column joints. The main focus of this research is to develop and evaluate the seismic behavior of RC beam-column joints rehabilitated with innovative technique. This method considers the real condition and physical constraint in joint regions. In order to study the behavior of the beam-column joints, nonlinear finite element analysis were performed using LS-Dyna software. In the present study three numerical models were developed and their outputs were compared to the experimental results carried out by past researchers. A finite element analysis has been conducted to study the seismic performance of exterior RC beam-column joints rehabilitated with New Scheme. The results from this numerical study demonstrated significant strength and ductility improvement in a Rehabilitated RC beam-column joint.

*Keywords: Rehabilitation; Beam-Column Joints; Seismic Performance; LS-Dyna Software*

## 1. INTRODUCTION

Damage incurred by earthquakes over the years has indicated that many reinforced concrete (R/C) buildings, designed and constructed during the 1960s and 1970s, were found to have serious structural deficiencies today, especially in their columns and beam-column joints. Such deficient joints have inadequate or absent joint transverse reinforcement and/or insufficient anchorage of the beam bottom reinforcement. The objective of beam-column joint rehabilitation is to strengthen the shear and bond-slip resistance in order to eliminate types of brittle failure and ensure instead that ductile flexural hinging in the beam will take place. Joints around the perimeter of the building are more vulnerable than the interior joints. Therefore assessment of exterior joint's performance would be more important. In the exterior joints, initial cracks around the embedment region proceeded diagonally toward the column bar splice region and extended downward to the bottom column, causing spalling of a large column piece and prying of the beam top bar, as shown in Fig. 1.1 (Tsonos, 2010, El-Amoury and Ghobarah, 2002).

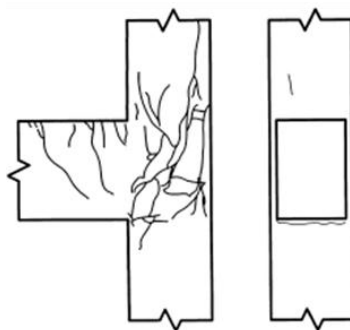


**Figure 1.1.** Typical cracking patterns of non-seismically detailed joints observed by Beres *et al.* (1991)

## 2. REVIEW ON BEAM-COLUMN JOINT MODELS

Many researchers have attempted to model the behaviour of RC beam-column joints following various approaches that include, lumped plasticity models, multi-spring models, finite element simulations and fracture mechanics based approaches. Some of the earliest work to simulate the inelastic response of reinforced concrete frames relied on the calibration of the plastic hinges within the beam-column line elements to introduce the inelastic action of the beam-column joint. Several geometric curves and rules, based on experimental data, defining the hysteretic behaviour of the connections were proposed. Townsend and Hanson (1973), Anderson and Townsend (1977) and Soleimani *et al.* (1979) suggested this approach. Finite element based models have also been utilized by several researchers to analyse beam-column joints. Nagai *et al.* (1996) used three dimensional non-linear finite elements to model a high strength concrete joint subjected to biaxial monotonic loading. The inelastic behaviour of interior wide column joints subjected to uniaxial loading has been investigated by Bing *et al.* (2003) using two dimensional non-linear finite elements. A finite element approach specially developed for detailed modelling of fracture in quasi-brittle materials has been proposed by Eligehausen *et al.* (2006) and also utilized by Sharma *et al.* (2008 and 2009).

## 3. MODELING

The beam-column joint considered for analysis studied by El-Amoury and Ghobarah (2002), consists of a cantilever portion and column portion. The column had a cross section of 400 mm x 250 mm with an overall length of 3000 mm and the beam had a cross section of 250 mm x 400 mm and the length of the cantilevered portion was 1750 mm. The beam-column joints are designed assuming that points of contra-flexure occur at the mid-height of columns and the mid-span of beams. The top longitudinal reinforcements in the beam are bent down into the column, whereas the bottom reinforcement was anchored 150 mm from the column face. No transverse reinforcement was installed in the joint region. The beam was reinforced using 4#20 as top and bottom longitudinal bars and #10 as transverse steel. The column was reinforced with 6#20 plus 2#15 as longitudinal bars and #10 ties spaced 200 mm. The dimensions and reinforcement details of all of the specimens are identical, as shown in Fig. 3.1.

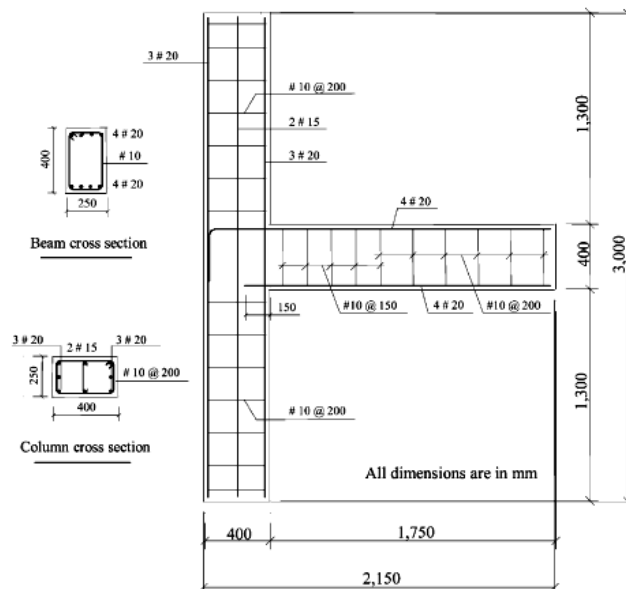


**Figure 3.1.** Specimen dimensions and reinforcement details tested by El-Amoury and Ghobarah (2002)

### 3.1. Boundary Conditions

The boundary conditions are set in the model to mimic the experimental test conditions. Both ends of the column were hinged. The bottom of the column is restrained in three (3) degrees of freedom at the

$U_x$ ,  $U_y$  and  $U_z$  directions. In this modeling, the column is allowed to rotate at the  $R_y$ .

### 3.2. Material model

The material model WINFRITH\_CONCRETE (MAT\_84) available in LS-DYNA is utilized in the present study to model concrete.

Material model PLASTIC\_KINEMATIC (MAT\_003) is used to model steel. It is an elastic-plastic material model with strain rate effect.

### 3.3. Loads

In order to incorporate the gravity and cyclic loads in FE Model, two steps are defined in the FE simulation. The gravity load is simulated in the first step as a uniform pressure equal to  $6 \text{ N/mm}^2$  applied at top of the column, and was approximately equal to  $0.2f'_c$ , where  $f'_c$  is the compressive strength of concrete. The lateral horizontal load is incorporated in the second step of the FE analysis as a monotonic incremental displacement applied tangential to the end of the beam until failure of the specimen.

### 3.4. The Finite Element Mesh

In order to obtain accurate results from the FE model, the size of the element meshing is set to 3 cm. The mesh element for concrete and rebar are 3D solid, 2D truss, respectively. Fig. 3.2. and Fig. 3.3. shows the meshed structure for the beam-column joint model.

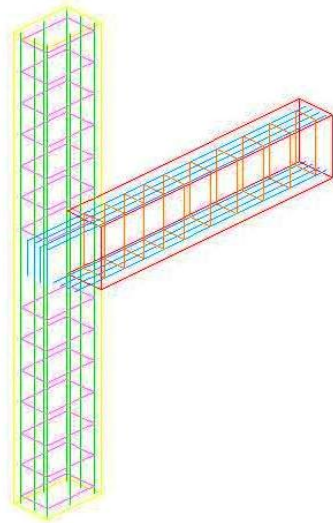


**Figure 3.2.** Typical view of LS-Dyna model

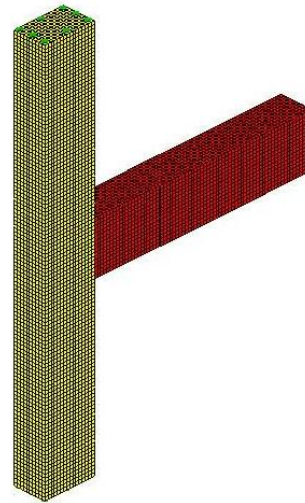


**Figure 3.3.** Typical meshed control specimen

## 4. VALIDATION OF THE NUMERICAL MODEL WITH EXPERIMENTAL RESULT

In order to validate the accuracy and reliability of the aforementioned numerical model, a numerical analysis of a full scale RC beam-column under seismic loads was performed and its results were compared with the test and numerical results reported by El-Amoury and Ghobarah (2002).

### 4.1. Tests by El-Amoury and Ghobarah (2002)

El-Amoury and Ghobarah (2002) performed cyclic tests on exterior beam-column joints that represented the joints built in accordance with pre-1970's codes. Though, the tests were conducted with an aim to verify the seismic rehabilitation scheme using GFRP sheets, one control specimen

named 'T0' that had gravity load design details is considered in this study. There was no transverse reinforcement within the joint core, and the beam's longitudinal bottom bars were embedded only to a length of 150 mm from the face of the column. A constant axial load of 600 kN was applied on the column that represented approximately 20% of the column's load carrying capacity.

When the specimen was pushed up, the bond-slip cracks opened and the lateral load-carrying capacity deteriorated significantly; however, when it was pulled down, the diagonal shear cracks opened. This caused disintegration of the concrete, deterioration of the bond condition of the beam top bars and degradation of the lateral load-carrying capacity. The specimen reached a maximum load of 60.0 kN up and 86.0 kN down, which is much less than the expected theoretical load at first steel yield of approximately 110.0 kN, as shown in Fig. 4.1. The test was halted at displacement of 50 mm as the load-carrying capacity was greatly reduced. In effect, when pushing up on the beam, bond slip failure of the beam bottom reinforcement occurred and when pulling down, joint shear failure occurred. The final failure pattern is shown in Fig. 4.2.

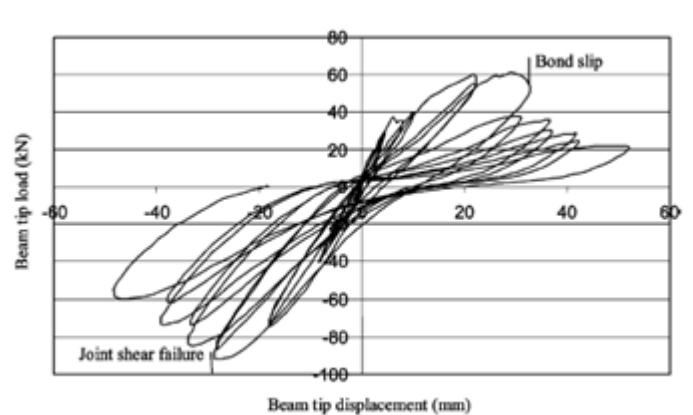


**Figure 4.1.** Beam-tip load-displacement of specimen T0 (El-Amoury and Ghobarah, 2002)

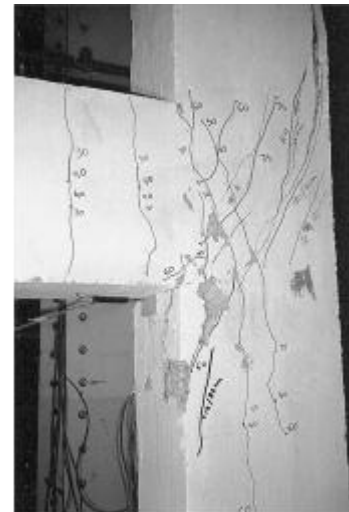


**Figure 4.2.** Failure pattern of specimen T0 (El-Amoury and Ghobarah, 2002)

## 5. FE NUMERICAL RESULTS

This section presents the output results of the LS-DYNA FE model analysis. A FE model runs for three different cases to simulate the actual specimens that were tested in the experimental program. In the following sections, the load-displacement curve and stresses will be discussed for the following cases:

1. Control specimen (CS-1).
2. Control specimen (CS-2).
3. Retrofitted specimen with mechanical anchorage using steel plates and threaded rods (RS).

### 5.1. Control Specimen (CS-1)

The first control specimen was detailed with discontinuous beam's bottom reinforcement rebars and no confinement stirrups within the joint region.

#### 5.1.1. Load-Displacement Curve

The load-displacement curve is generated numerically in the FE model analysis at the end of the beam. Fig. 5.1. Shows the FE model load-displacement curve for the control specimen.

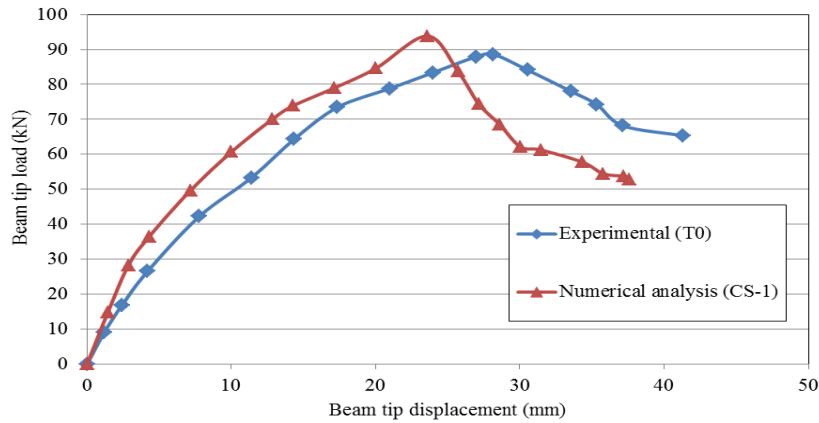


**Figure 5.1.** FE model load-displacement curve for control specimen (CS-1), and validation of model with tests performed by El-Amoury and Ghobarah (2002)

In this section, the comparison between the load-displacement curve for experimental and FE model is presented in Fig. 5.1. The results from the FE numerical analysis show an overall good agreement with the experimental test data. In the linear range, the specimen stiffness in the numerical analysis is slightly greater than the actual specimen. The main reasons for this difference are: 1- due to few assumptions in the material properties due to insufficient data. 2- The behavior of the actual supporting system is not identical to the boundary conditions in the FE model. 3- The presence of micro-crack in the concrete due to shrinkage and temperature change from the day of pouring until the day of testing. 4- The assumption of full bond with no slippage between the embedded reinforcement rebars and the concrete core in the FE model, but in actual specimen there is always some slippage when the rebar elongates under the subjected loads.

### 5.1.2. Stresses

Stresses are calculated through the step increments of the lateral loading phase. The specimen failure is attributed to shear strength degradation in the joint region. This shear failure is due to a combination of two failure mechanisms; (i) tension cracking and (ii) compression crushing of the concrete at the joint area. The concrete shear stresses Von-Mises in the beam-column joint specimen and the axial force in the reinforcing rebar are shown Fig. 5.2. and Fig. 5.3. Respectively.

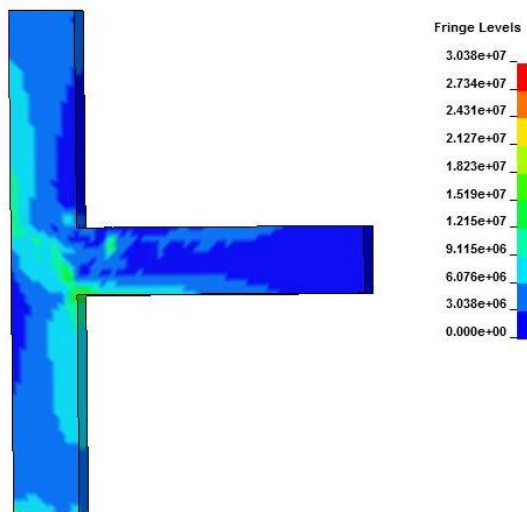


**Figure 5.2.** Von-Mises stresses in Specimen CS-1

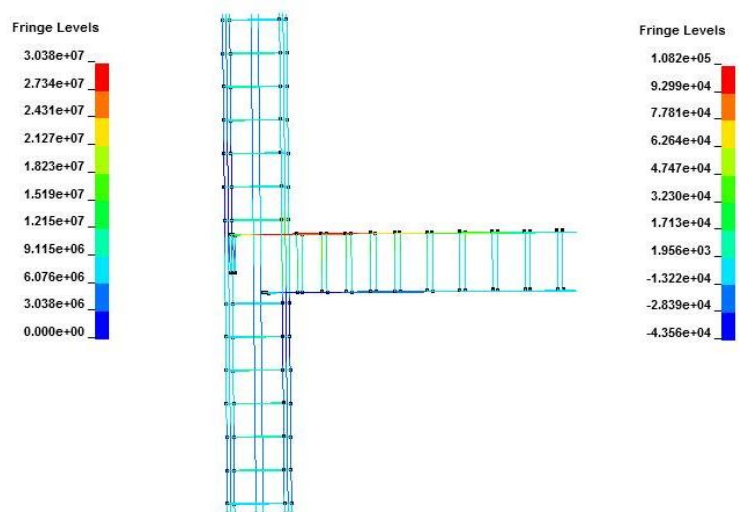


**Figure 5.3.** Rebar axial force in specimen CS-1

## 5.2. Control Specimen (CS-2)

The second control specimen was designed according to ACI 318-08 code. The objective of the numerical analysis of control specimen (CS-2) was to set as a baseline for comparing between behavior of exterior RC beam-column joint designed per current ACI 318-08 code requirements and retrofitted specimen (RS).

### 5.2.1. Load-Displacement Curve

The curve shows the lateral load increases linearly until 98 kN after which non-linearity is initiated. In the non-linear portion of the curve, the specimen has reached a maximum lateral load equal to 113 kN with a 33 mm lateral displacement. After reaching the peak point, strength degradation is initiated in the joint specimen that continued until the end of the numerical run.

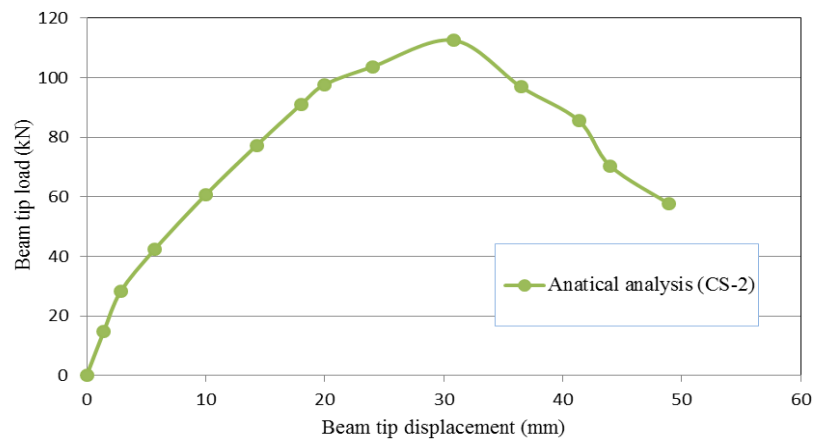


Figure 5.4. FE model load-displacement curve for control specimen (CS-2)

### 5.2.2. Stresses

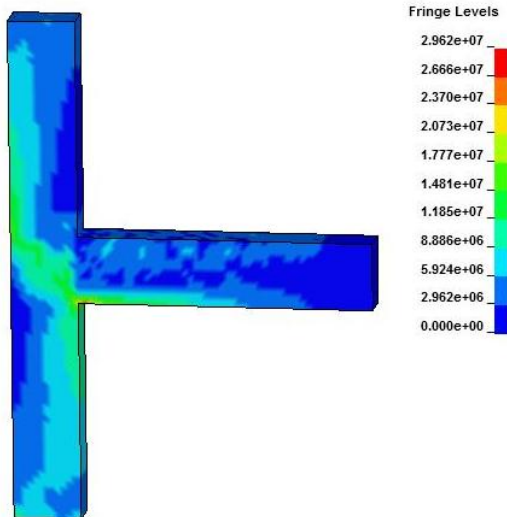


Figure 5.5. Von-Mises stresses in specimen CS-2

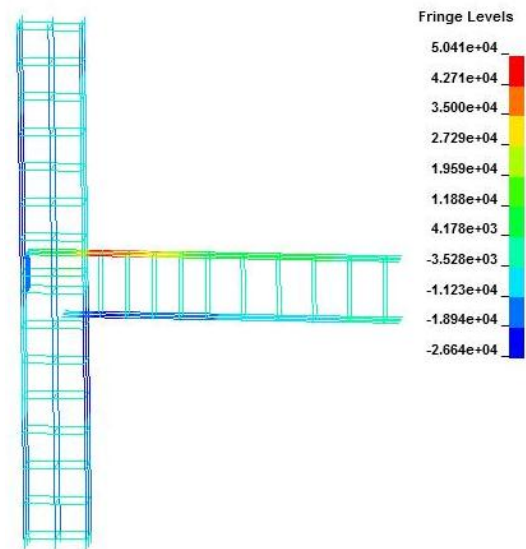
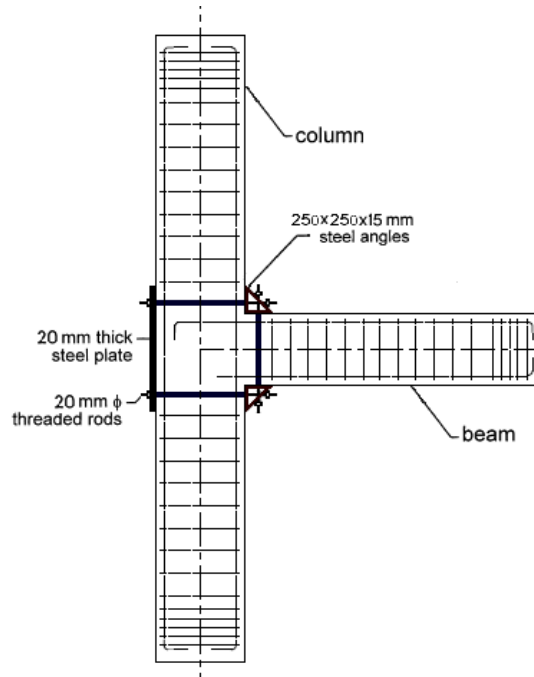


Figure 5.6. Rebar axial force in specimen CS-2

As a conclusion, the specimen exhibited somehow a ductile mode of failure since the degradation in load strength was not as severe as happened in the deficient joint.

### 5.3. Retrofitted Specimen

The proposed rehabilitation schemes consist of mechanical anchorage using steel plates and rods. The bracing system is divided into three steel units, as shown in Fig. 5.7. In order to make the steel encasement of the beam and column possible, no holes were drilled through the specimen. The three steel units were then mounted and held in place using high tensile strength rods. The system proved to be versatile since it could be easily installed for exterior and interior beam-column joints, even in the presence of a slab, with additional simple perforations. It can improve the bond slip behavior, so that the penetration length of beam bars into the column can be reduced.



**Figure 5.7.** Retrofitting schemes: specimen RS

The size and reinforcement details of strengthened specimens were identical to the control specimen except the enlarged area.

#### 5.3.2. Load-Displacement Curve

The curve shows the lateral load increases linearly until 98 kN after which non-linearity is initiated. In the non-linear portion of the curve, the specimen has reached a maximum lateral load equal to 122 kN with a 33 mm lateral displacement. After reaching the peak point, strength degradation is initiated in the joint specimen that continued until the end of the numerical run.

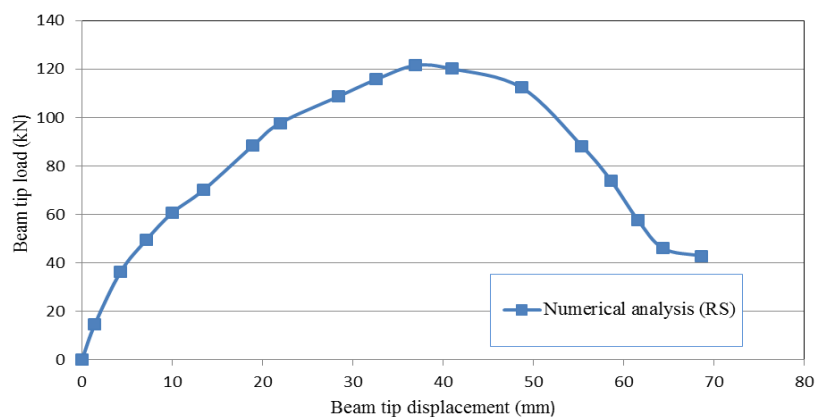


**Figure 5.8.** FE model load-displacement curve for specimen (RS)

### 5.3.3. Stresses

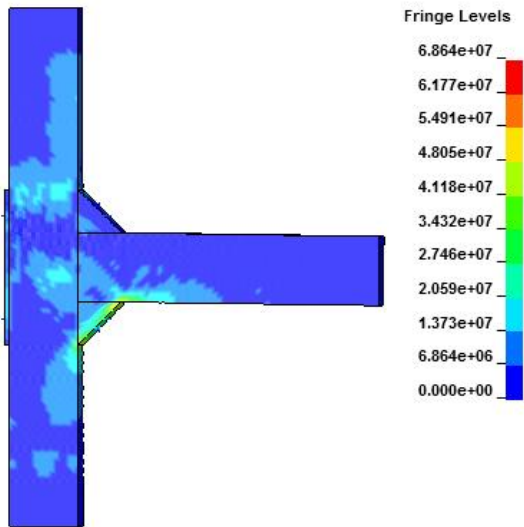


Figure 5.9. Von-Mises stresses in specimen RS

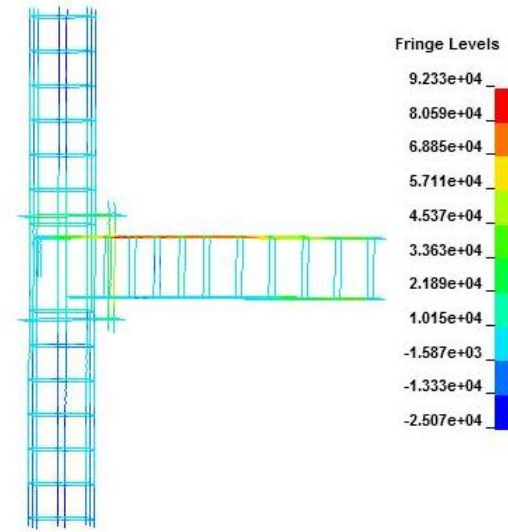


Figure 5.10. Rebar axial force in specimen RS

## 6. CONCLUSIONS

Based on the LS-DYNA modeling and analysis carried out on the control and retrofitted beam column joint specimens, the following conclusions were drawn:

- 1- Fig. 6.1. Shows the load-displacement curve for the specimens CS-1, CS-2 and RS. The Specimens failed at an average load of 93 kN, 113 kN and 122 kN respectively. Specimen CS-2 showed almost 20% increase in the load-carrying capacity compared with specimen CS-1. Specimen RS reached a higher load level and maintained the load-carrying capacity at displacement levels much higher than those of the other two specimens.

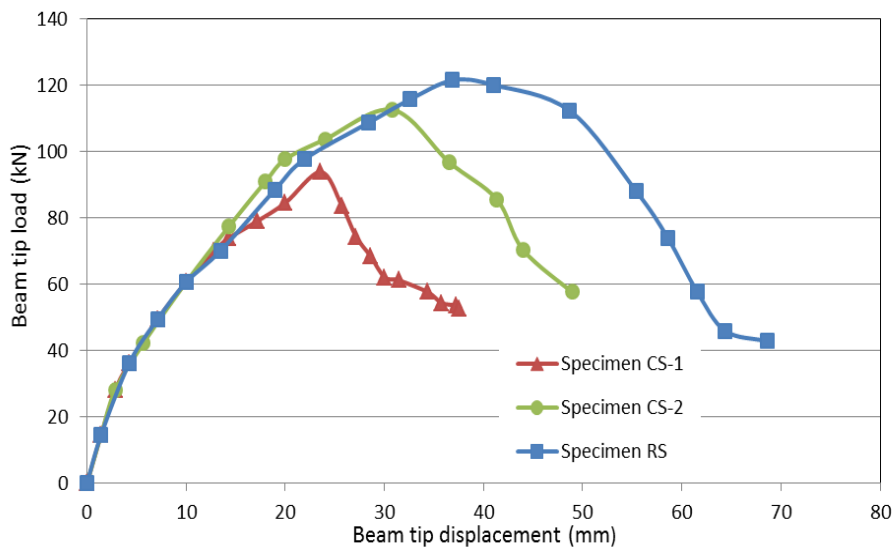


Figure 6.1. Comparison between Peak lateral load-Lateral displacements of specimens

- 2- The joint enlargement an effective method to reduce shear stress transmitted in the joint panel. The failure mode can also be changed from brittle joint shear failure to flexural failure in beams, indicating the relocation of plastic hinge from column face to the edge of enlargement.
- 3- The study shows that an appropriate numerical simulation of upgraded specimens can be able to predict a considerably close response as that was obtained from the experimental studies.
- 4- The rehabilitation scheme was found to be effective, simple to install and non-disruptive to the function of the building.

## REFERENCES

- American Concrete Institute (ACI). (2008). Building Code Requirements for Structural Concrete and Commentary. *ACI Committee 318*. ACI 318-08.
- Anderson, J.C. and Townsend, W.H. (1977). Models for RC frames with degrading stiffness. *Journal of the Structural Division, ASCE* **103:12**, 2361-76.
- Beres, A., Pessiki, S.P., White, R.N. and Gergely, P. (1991). Seismic Performance of Existing Reinforced Concrete Frames Designed Primarily for Gravity Loads. *Sixth Canadian Conference on Earthquake Engineering*. 655-662.
- Bing, L., Yiming, W. and Tso-Chien, P. (2003). Seismic behavior of non-seismically detailed interior beam-wide column joints. Part II: Theoretical comparisons and analytical studies. *ACI Journal* **100:1**,56-65.
- El-Amoury, T. and Ghobarah, A. (2002). Seismic rehabilitation of beam-column joint using GFRP sheets. *Engineering Structures: The Journal of Earthquake, Wind and Ocean Engineering* **24:11**,1397-1407.
- Eligehausen, R., Özbolt, J., Genesio, G., Hoehler, M.S. and Pampanin, S. (2006). Three Dimensional Modeling of Poorly Detailed RC Frame Joints. *Proceedings of the Annual NZSEE Conference*. Paper No. 23.
- Nagai, T., Kashiwazaki, T. and Noguchi, H. (1996). Three Dimensional Nonlinear Finite Element Analysis of RC Interior Beam-Column Joints With Ultra High-Strength Materials under Bi-directional Load. *Japan Concrete Institute*. Paper No. 476.
- Sharma, A., Genesio, G., Reddy, G.R. and Eligehausen, R. (2009). Nonlinear cyclic analysis using microplane model for concrete and bond slip model for prediction of behavior of non-seismically detailed RCC beam-column joints. *Journal of Structural Engineering* **36:4**,250-7.
- Sharma, A., Reddy, G.R., Vaze, K.K., Ghosh, A.K., Kushwaha, H.S. and Eligehausen, R. (2008). Investigations on inelastic behavior of non-seismically detailed reinforced concrete beam-column joints under cyclic excitations. *BARC external report no. BARC/2008/E/017*.
- Soleimani, D., Popov, E.P. and Bertero, V.V. (1979). Nonlinear Beam Model for RC Frame Analysis. *7th ASCE conference on electronic computation*. pp. 483-509.
- Townsend, W.H. and Hanson, R.D. (1973). Hysteresis Loops for Reinforced Concrete Beam-Column Connections. *Proceedings of 5th World Conference on Earthquake Engineering*. **Vol I**: 1131-4.
- Tsonos, A.G. (2010). Performance enhancement of R/C building columns and beam-column joints through shotcrete jacketing. *Journal of Engineering Structures* **32:3**,726-740.